Development of Electric Field Stress Control Devices for a 132 kV Insulating Cross-arm using Finite Element Analysis

Christos Zachariades, Simon M. Rowland, *Fellow, IEEE,* I. Cotton, *Member, IEEE,*
Vidyadhar Peesapati and David Chambers

***Abstract*— Insulating cross-arms (ICA) allow compaction or upgrading of transmission lines. The process of designing and verifying the performance of electric field grading devices is reported for rigid cross-arms on a 132 kV lattice tower. For the grounded end, traditional grading devices resembling rings which follow the general shape of the insulators were designed. For the high-voltage (HV) end, an iterative process yielded a novel grading device which is a unibody piece of cast aluminium that manages the field on all four ICA members. Finite element analysis (FEA) simulations show that the electric field magnitude at the triple junctions of the insulating members meet the design criteria of 3.5 kV/cm. Also the field magnitude on the metallic end-fittings and electric field grading devices is maintained below 18 kV/cm. The corona extinction test was performed on ICA assemblies showing that the grading devices can effectively control the electric field at voltages of up to 132 kV since the average corona extinction voltage was 173.7 kV, well above the required value. The complete ICA assemblies were installed on an existing line in Scotland in August 2013. This paper provides a set of recommendations for use of FEA in the design of complex insulation geometries.**

***Index Terms*— composite insulators, cross-arms, FEA, ICA, insulating, overhead lines, towers.**

I. INTRODUCTION

A novel insulating cross-arm (ICA) has been developed for new and existing overhead transmission lines operating at 132 kV and above. The ICA can be used to either directly replace the steel cross-arms and insulators on existing lattice towers to enable the upgrading of existing infrastructure or for building new towers with smaller footprint than otherwise possible. The cross-arm consists of four insulating members, end fittings, field grading devices and a nose connection for the attachment of the conductor (Fig. 1). The two main structural elements of the assembly, the compression insulators, have a unique non-cylindrical geometry which gives them improved mechanical characteristics compared to conventional overhead line insulators. Specifically, the profile of a compression insulator is based on a patented T-shaped column section which exhibits a substantially increased second moment of area when compared to a cylindrical profile of the same cross-sectional area. This design allows for a 2.4 times weight reduction for the compression insulator while allowing the cross-arm to be installed in a similar manner to conventional steel lattice cross-arm, i.e. at shallow raking angles, without using any diagonal bracing [1].

Designing electric field stress management devices for the ICA presented unique challenges. The cross-sectional shape of the compression insulators and their end-fittings, the method of attachment of the end-fittings to the insulators and the proximity of the insulating members to each other at the nose end of the cross-arm meant that traditional solutions would not work effectively for the ICA. Separate corona rings for each insulating element, for example, are not possible.

The purpose of the study presented is to advance the development of new grading devices through finite element analysis (FEA) simulations of electric fields. For traditional insulators it is possible to exploit the rotational symmetry they exhibit along their longitudinal axis and use two dimensional analysis to simplify the electric field calculation [2]. The end-fitting of the compression insulator of the ICA however has to

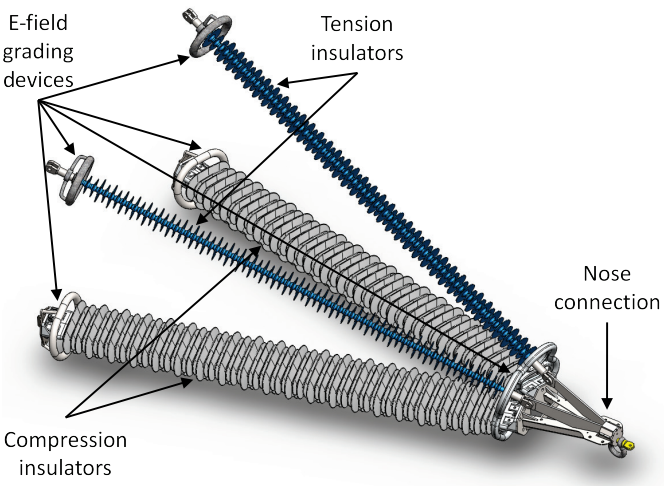

Fig. 1. The insulating cross-arm. It consists of four insulating members end fittings, electric field grading devices and a nose connection for the attachment of the conductor.

This work was supported by Scottish and Southern Energy Power Distribution and by National Grid.

C. Zachariades is now with the University of Manchester and High Voltage Partial Discharge Ltd, Salford, M50 2UW, UK (e-mail: christos@hvpd.co.uk).

S. M. Rowland (e-mail: s.rowland@manchester.ac.uk) and I.Cotton are with the University of Manchester and Arago Technology.

V. Peesapati is also with the University of Manchester.

D. Chambers is with Arago technology.

follow closely the shape of the core. The unconventional shape of the fitting results in different radii on its surface which result in complex special distributions of electric field. Furthermore the metallic components at the high voltage end of the ICA change the electric field distribution significantly when compared to a standard insulator. For these reasons, the simulations required the use of three-dimensional models.

II. Electric Fields On Composite Insulators

The electric field distribution on the surface and within polymeric insulators influences their short term and long term performance. The field along the insulators is not uniform with its magnitude being higher near the ends. The main factors that affect the field distribution are the line voltage, the shape of the insulator, the dielectric properties of the materials, the dimensions and position of grading devices and other line hardware as well as the orientation of the insulator with respect to the conductors [3].

A. Consequences of high fields on insulator aging

High electric fields under wet conditions, exceeding the water drop corona threshold of 4.4 kV/cm, can enhance corona activity on the surface of the insulator and accelerate aging of the material [4]. Corona can, for example, lead to generation of hydrophilic hydroxyl groups (-OH), and white deposits on the surface of corona-aged insulators [5]. Prolonged exposure to corona can result in the loss of hydrophobicity in addition to the development of cracks on the material surface which can degrade the performance of the insulator [6].

When contaminated and wet, an insulator can experience increased leakage current flow on its surface. As a result, discharges of hundreds of milliamps may develop on the surface, a phenomenon known as dry-band arcing. Such discharges can result in surface ageing and lead to flashover [7].

B. Corona from metallic hardware

If not controlled properly, corona from the metallic insulator hardware can produce radio interference and audible noise [3]. The field distribution and magnitude can be controlled by the position and geometry of the end-fittings and grading rings [8]. Improper dimensioning and positioning can result in corona cutting, in which corona discharges originating from the metallic parts of the insulator degrade the shed material [9]. In severe cases this erodes the silicone, exposing the core, leaving it vulnerable to acid attack.

Furthermore, the design of the end fittings of insulators can have a detrimental effect on the electric field distribution near the triple junction, the point where the housing, the core and the metal work meet. If the insulator is not well designed, discharges at this critical location can erode the sealing material that keeps the insulator watertight [10].

In the case of the ICA, managing the electric field near and around the composite cross-arm assembly is particularly critical. The compaction of the overhead line, which is one of the main benefits of the technology, has the effect of reducing phase-to-phase and phase-to-tower spacing when compared to traditional lines for the same voltage. In turn this can increase voltage gradients on conductors and metal fittings which can increase the probability of flashover and occurrence of audible noise [11].

C. Design Requirements

The importance of the electric field distribution along a composite insulator has been recognized by the industry. For example, in the UK, National Grid has set specific criteria as part of their technical specifications that an OHL insulator must meet before it can be installed on their network [12]. These criteria coincide with the recommendations of the IEEE taskforce on Electric Fields and Composite Insulators [3] and EPRI [13]. These requirements have been adopted for the ICA. In summary these are:

- Maximum electric field magnitude on the sheath and sheds measured 0.5 mm from the surface: 4.5 kV_{rms}/cm.
- Maximum electric field magnitude at the triple junction: 3.5 kV_{rms}/cm.
- Maximum electric field magnitude inside the core and weather-shed material: 30 kV_{rms}/cm.
- Maximum electric field magnitude on metallic end-fittings and electric field grading devices: 18 kV_{rms}/cm.

III. Finite Element Analysis

As an alternative to experimental methods, the electric field can be studied using numerical techniques. The most popular are the charge simulation method (CSM), the boundary element method (BEM) and the finite element method (FEM). In this case, the study of the electric field distribution and the development and optimization of grading devices for the ICA were performed using the FEM.

A. The Finite Element Method

The FEM is a numerical method for solving mathematical models which are too complex or cannot be solved analytically. It is used to investigate various properties of components or assemblies and predict how they will behave under external stresses. Computer-based simulations that utilize the FEM can be employed to transfer design iterations into the virtual domain, leaving the manufacturing of prototypes for final design verification only [14].

The method works by splitting the physical model into a large number of small elements of simple geometric shape, the finite elements, to enable the representation of complicated geometries in a piecewise continuous manner. The application of the FEM requires knowledge of the partial differential equations (PDE) that govern the physics of the problem, the boundary conditions at the edges of the regions of interest and the material properties of the object. The PDE are approximated by simpler linear or quadratic functions [15].

B. FEA of Electrostatic Fields

In power systems, because of the alternating voltage, the electric field changes with time. However, its frequency is

relatively low. As a result, when considering its effects it can, in this case, be treated as an electrostatic field.

In electrostatics, the electric field is irrotational and arises from a voltage gradient or potential difference, and can therefore be expressed as the gradient of the electric potential φ:

$$\vec{E} = -\nabla\varphi \tag{1}$$

Its calculation can be derived from an Interior Boundary Value Problem (IBVP) subject to appropriate boundary conditions by solving Laplace's equation:

$$\nabla^2\varphi = 0 \tag{2}$$

On boundaries that are perfect conductors the Dirichlet boundary condition applies:

$$\varphi = V \tag{3}$$

where V is a constant.

On all other surfaces the Neumann boundary condition applies:

$$\frac{d\varphi}{dn} = 0 \tag{4}$$

where n is the direction normal to the surface.

The unknowns can be found by minimising the energy functional. The energy functional takes its minimum value only if the potential φ is a solution to Laplace's equation and satisfies the boundary conditions. This can be expressed as:

$$\frac{\partial W}{\partial \varphi} = 0 \tag{5}$$

where W is the energy stored in the electric field within an area S and is given by:

$$W = \frac{1}{2}\varepsilon_r \int_S \left|\vec{E}\right|^2 dS = \frac{1}{2}\varepsilon_r \int_S \left|-\nabla\varphi\right|^2 dS \tag{6}$$

The virtual parts of the model have exactly the same dimensions as the actual parts used for fabricating the cross-arm. Some of the features of these parts, such as bolt holes on the metal work, have been suppressed to further reduce the complexity of the model and speed up the computation. Experience and experimentation determines which parts of a model can be suppressed without sacrificing accuracy.

IV. Simulation Setup

A. Reference Model

To identify where the areas of high electric field magnitude are located on the cross-arm, a model consisting of all the metallic hardware at the HV-end of the ICA and a full 132 kV compression insulator was assembled in SolidWorks. The second compression insulator as well as the tension insulators were excluded from the model since it was not possible to simulate the entire assembly with the hardware available while keeping the element size within acceptable limits to achieve the appropriate accuracy. This approach was deemed sufficient for two reasons. Firstly, the tension insulators are off-the-shelf products and as such they have undergone all relevant testing to be certified for operation on a network. Secondly, as will be demonstrated subsequently, the determining factor for the electric field magnitude is the dimensions of the metallic nose cone, primarily near the triple junction, which are much smaller than those of the components omitted. The reason for this is that the distance between the conductor and the insulator surface is much larger than for a traditional insulator due to the presence of the nose cone. The proximity of the four insulating members to each other at the HV-end also helps to even out the electric field distribution. In addition, due to the relatively small dimensions of the metallic hardware at or near the areas of interest (e.g. the triple junction), other hardware with larger dimensions (especially ones that have bigger radii e.g. the conductor) do not have as much influence on the local electric field magnitude as they do for traditional insulators.

The model was the imported into COMSOL Multiphysics, a commercial FEA software package. For the mesh, special attention was given to preserve the radii of the metallic components, especially the ones on the compression insulator end-fittings which are rather small, of the order of 1 mm.

By manually meshing the relevant surfaces, it was made sure that at least two second-order elements were used per 90° arc to maintain the discretization error below 0.1% [16]. The mesh parameters for the model were the following:

- Number of elements: 21 248 656 (tetrahedral)
- Minimum element size: 0.0006 m
- Maximum element size: 0.24 m

The computational domain for the simulation was set to be a $4\text{ m} \times 3\text{ m} \times 3\text{ m}$ box containing the simplified model. To further decrease the complexity and increase the speed of the computation, the OHL tower was not included. Instead, the rightmost plane of the box played the role of the tower. The other sides of the box were given sufficient clearance from the model to not affect the result of the simulation. The cross-arm assembly was placed 10 cm away from the tower plane to account for the bracket that is normally used to fasten the cross-arm to the tower. The computation domain can be seen in Fig. 2.

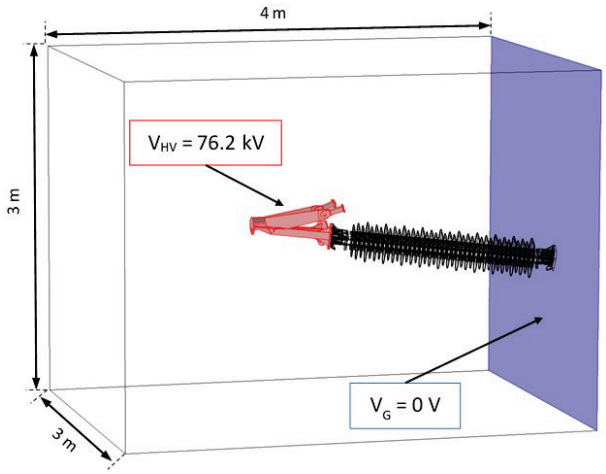

Fig. 2. Computation domain with 132 kV ICA model. The right-most surface of the domain is grounded to represent the tower which is omitted to simplify the calculation.

The only material property that is taken into account for the electrostatic field calculation is the permittivity. The metallic components were simulated by setting their surfaces to a fixed voltage. The materials and corresponding permittivities used for the simulation are summarized in Table I.

The boundary conditions used for the simulation were:

- HV metallic hardware surfaces: 76.2 kV
- LV metallic hardware surfaces: 0 V
- Tower (rightmost) plane: 0 V
- Other internal surfaces: continuity
- Outer boundaries: zero charge

B. Simulation Results without Grading Devices

Figure 3 shows the results of the simulation in the form of electric field contours. The highest electric field magnitude of 20 kV/cm can be observed on the triple junction at the grounded end of the compression insulator. In other words, without grading, the field on the compression insulator greatly exceeds the 3.5 kV/cm limit. Furthermore, the result emphasizes the difference between the cross-arm and traditional OHL insulators where one would expect the highest electric field magnitude to be at the HV-end.

The difference can be attributed to two main factors. Firstly, the end-fitting of the compression insulator is very different geometrically from a standard long-rod insulator end-fitting since it needs to follow the unconventional shape of the insulator core. Secondly, the presence of other metallic hardware as well as the proximity of the end-fittings of the four insulators at the HV-end of the cross-arm help to even out the electric field distribution. This reduces the electric field magnitude at the HV-end of the compression insulator.

TABLE I
MATERIALS AND PERMITTIVITIES FOR ELECTRIC FIELD COMPUTATION

Part	Material	Permittivity (ε_r)
Nose cone	Steel	1.0
End-fitting	Aluminium	1.0
Core	Fiber Reinforced Plastic (FRP)	5.0
Shed/Sheath	Silicone Rubber (SiR)	3.5
Box	Air	1.0

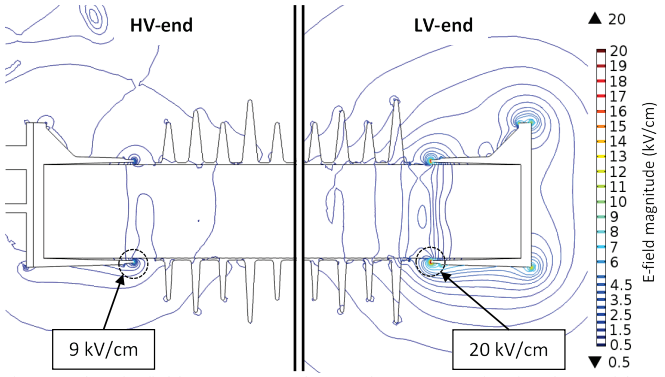

Fig. 3. Electric field contours on the 132 kV compression insulator without grading devices. The maximum electric field magnitude based on the simulation results is 20 kV/cm observed at the triple junction of the grounded end.

V. GROUNDED END GRADING DEVICE

A. Design

To bring down the magnitude of the field, a grading device was designed using SolidWorks. The device is not strictly a ring since its shape follows the outline of the compression insulator and its sheds (Fig. 4). It is made out of tubular aluminium with diameter of 26 mm. This specific diameter of tube was chosen for several reasons. First, the electric field magnitude around a ring with such a tube diameter is substantially lower than the corona inception voltage at 132 kV. Additionally, it can be fabricated with a tight enough radius that it can follow the general shape of the compression insulator without needing special manufacturing methods.

B. Position Optimisation and Simulation Results

The model of the grounded end grading device was imported into COMSOL and then integrated with the ICA model. The computation domain and boundary conditions were set to be exactly the same as in the previous section. To find the optimal position for the grading device a parametric study was conducted by varying the horizontal distance of the vertical plane of the grading device from the edge of the end-connection closest to the sheds (***d***) (Fig. 5). The parametric sweep was run with parameter ***d*** ranging from 0 to 70 mm in steps of 10 mm. The electric field was computed for each position of the grading device. The maximum electric field magnitude values were plotted against the value of parameter ***d*** and are presented in Fig. 6.

The electric field magnitude is reduced to acceptable levels at the triple junction area for two positions of the grading device. *Position A* is when the center of the device is directly on top of the triple junction. *Position B* is when the device is closest to the first shed of the insulator. The former position was preferred because of the increased risk of discharges from the device to the shed in *Position B* which could erode the silicone rubber in the long term. It was decided therefore to place the device directly in line with the triple junction.

The electric field distribution with the device at the optimal *Position A* is presented in the form of a contour plot in Fig. 7. The maximum electric field magnitude with the grading device is brought down to 3.5 kV/cm which is the limit for the triple junction. The maximum field magnitude on the device itself does not exceed 12 kV/cm.

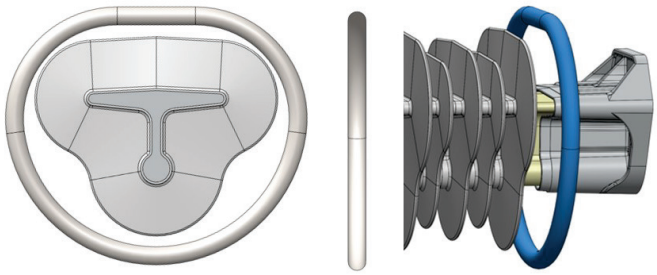

Fig. 4. Grounded end grading device for the compression insulator from different perspectives.

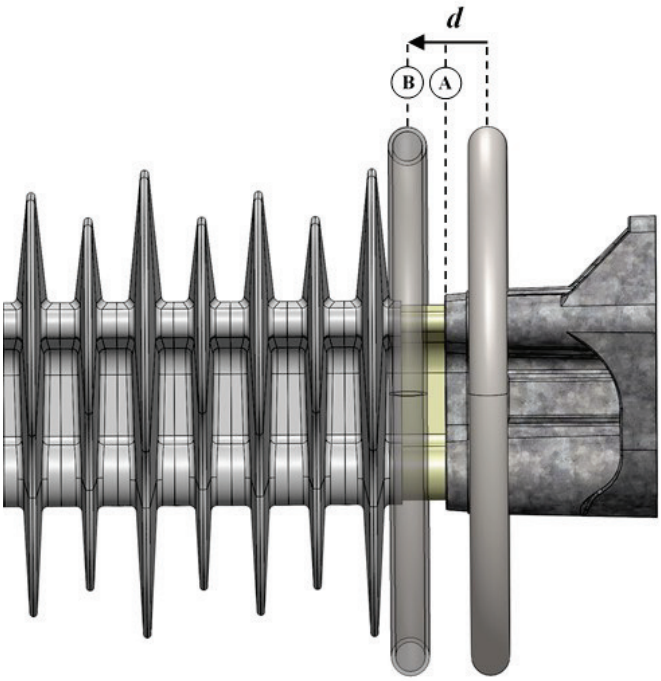

Fig. 5. Grounded end grading device position variation (parameter ***d***) and optimal positions A and B.

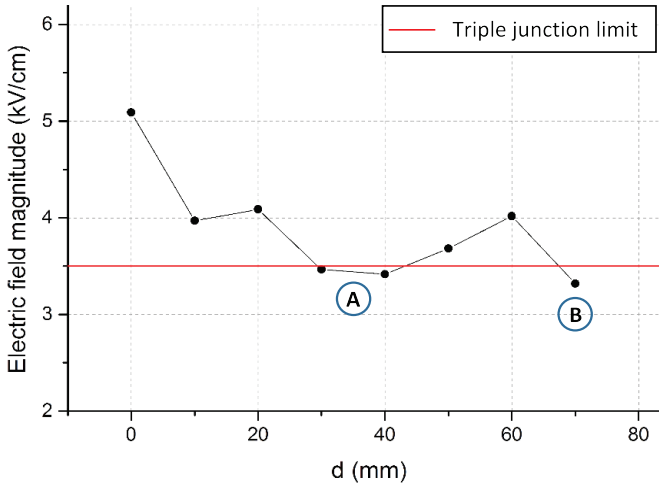

Fig. 6. Maximum electric field magnitude at the triple junction against the distance (d) of the grounded-end grading device from the edge of the compression insulator end-fitting. At positions A (30 mm - 40 mm) and B (70 mm) the electric field magnitude is reduced below the 3.5 kV/cm limit.

VI. High-Voltage End Grading Device

A. Design

At the HV-end of the cross-arm assembly the four insulators meet at the nose cone which facilitates the attachment of the conductor. The proximity of the four insulators at this area of the assembly makes it impossible to install an individual grading ring for each member. Additionally, as with the grounded end grading device, the geometry of the HV grading device has to be tailored to the unique shape of the compression insulator end-fittings. Hence, it was decided that it would be more effective to develop a solution that could manage the electric field around all four insulating members collectively.

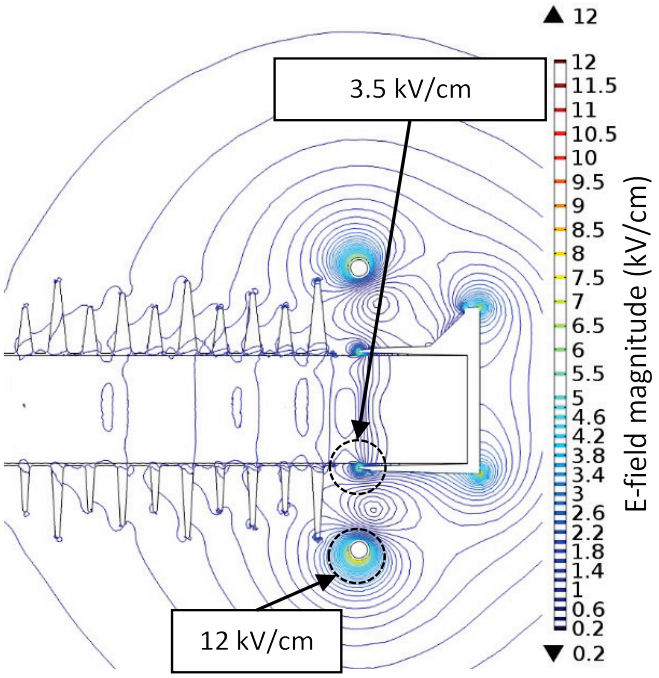

Fig. 7. Electric field contours for the grounded end with grading device. Maximum electric field magnitude at the triple junction is 3.5 kV/cm; maximum electric field on the grading device is 12 kV/cm.

The design methodology used for the grounded end grading device was initially considered for use as the HV end grading device. Two different devices fabricated from interconnected tubular components were designed and simulated. It quickly became apparent that with these devices the electric field magnitude at the triple junction could not be reduced to acceptable levels. This was primarily because the distance between the tubular sections of the device and the end fitting could not be reduced further if the device was to be able to physically fit between the four insulating members during installation. Furthermore, the tight bending radii of the tubular sections would require special manufacturing techniques, which would make the device difficult and expensive to produce.

To overcome the aforementioned limitations, a novel grading device was designed. The HV-end grading device was conceived to be a unibody piece of aluminium with holes of appropriate shape and size inside of which the end-connections of the four insulators would fit (Fig. 8). It has smooth rounded surfaces facing the insulators while its other

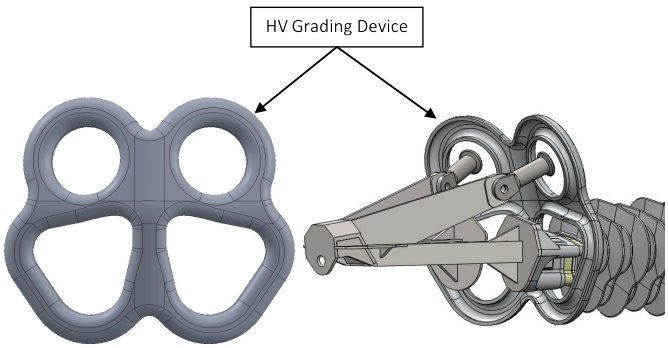

Fig. 8. HV grading device for the 132 kV ICA

side, facing the conductor, is concave to make it lighter, cheaper and easier to manufacture. Because of its shape, the device can be cast, reducing the cost of making multiples of the device. The most expensive stage of manufacturing is the construction of the mould which only happens once at the initial stages of the process. The device is fastened directly to the nose cone, ensuring an electrical connection to the HV while not interfering with any of the four insulator end-fittings.

B. *Simulation Results*

As before, the grading device was integrated with the 132 kV ICA model and imported into COMSOL. The electric field computation was carried out using the same parameters specified earlier. Since the simulation for the grounded end grading device showed that the best position for a grading device is directly above the triple junction, this result was adopted for the HV device as well. The electric field contours, taken on a plain running through the middle of the compression insulator, and the maximum electric field magnitude values at the HV-end of the ICA with the HV grading device in position are shown in Fig. 9.

The HV grading device manages to control effectively the electric field around the triple junction at the HV-end of the insulator reducing its magnitude to 2.9 kV/cm which is below the 3.5 kV/cm threshold. Also the field magnitude on the device itself does not exceed 6.7 kV/cm which is within the acceptable values, well below 18 kV/cm.

VII. Electric Field on the Compression Insulator

After integrating both grading devices with the ICA model and using the same simulation setup, the electric field was computed for the entire compression insulator. Figure 8 shows two plots of the electric field magnitude for the insulator. The red is plotted on a line 0.5 mm from the surface of the sheath of the insulator. The blue is plotted on a line inside the core. The field on the surface of the insulator does not exceed 1.9 kV/cm while the field in the core remains below 1.6 kV/cm. Both results are well within the acceptable limits defined in *Section II.E*.

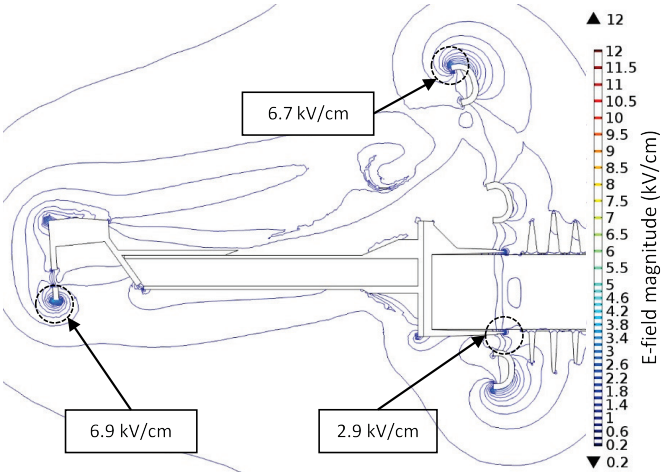

Fig. 9. Electric field contours for HV-end with grading device. Maximum electric field magnitude at the triple junction is 2.9 kV/cm; maximum electric field on the grading device is 6.7 kV/cm.

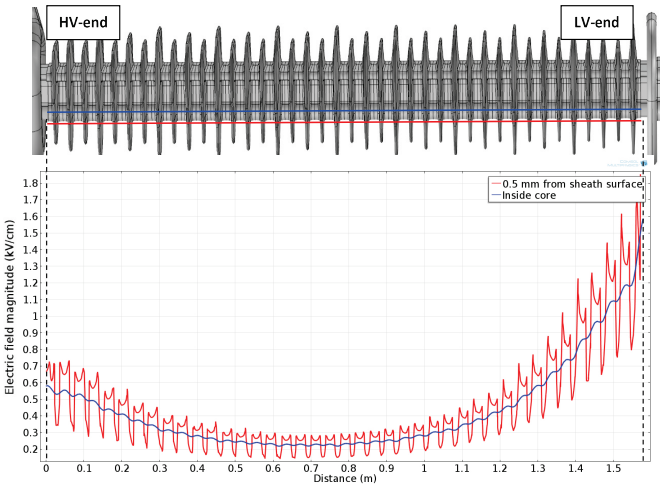

Fig. 10. Electric field magnitude on the surface and inside the core of the compression insulator at 132 kV.

VIII. Corona Extinction Test

To verify the capability of the electric field grading solution, prototypes of the devices were manufactured and installed on a 132 kV ICA. Since it is difficult to practically measure the electric field, the cross-arm was subjected to the corona extinction test in the HV laboratory of the University of Manchester.

A. *Requirements and Test Setup*

The corona extinction test is used to establish the voltage at which corona discharges are no longer visible on an insulator and its fittings. For the ICA the test was adapted from the Technical Specifications of National Grid, specifically the TS 3.4.17 [17]. The minimum allowable corona extinction voltage for transmission line insulators, and consequently for the ICA, are 110 kV for the 132 kV ICA.

The ICA was installed on a lattice tower section within the laboratory. The nose cone was fitted with a standard 132 kV conductor shoe and connected to the AC resonant test set using copper pipe. The pipe was terminated with a metallic sphere.

B. *Procedure*

After all electrical connections were made, the laboratory and control room were darkened completely and the observer was allowed 15 minutes to get accustomed to the conditions. The applied voltage was increased until corona was observed. It was then reduced slowly until no more discharges were visible at which point the voltage level was recorded. The procedure was repeated three times. The measured values were then corrected to the standard atmosphere [18].

C. *Results*

Corona discharges became visible at the conductor attachment point of the nose cone and on the outer rim of the HV grading device after the voltage exceeded 200 kV. Figure 11 shows a photograph of the cross-arm assembly captured with the UV camera after corona inception. Corona discharges can be seen in green and black, with black being more intense.

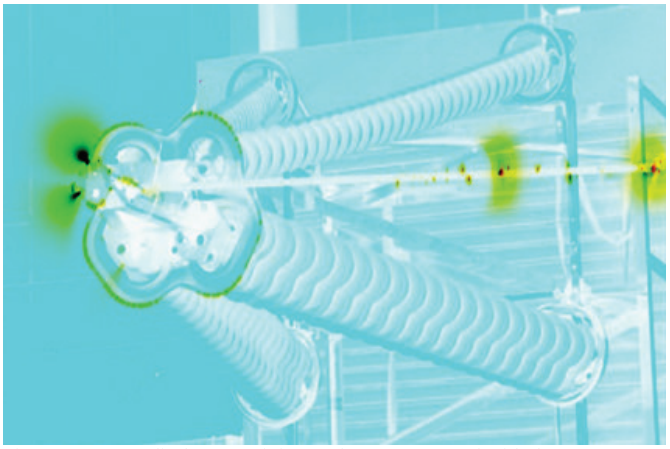

Fig. 11. Corona discharge activity on the ICA captured with the UV camera. The more intense discharges can be seen at the conductor attachment point and the rim of the HV grading device.

These observations coincide with the results of the FEA since the more intense corona activity can be seen at the locations where the highest electric field magnitude was calculated i.e. the rim of the HV grading device and the conductor attachment point.

The observed and corrected corona extinction voltage values are presented in Table II. The average corona extinction voltage was 173.7 kV i.e. 58 % higher than the 110 kV requirement for the 132 kV ICA. The test results, although not directly comparable with the simulation results, affirm the ability of the grading devices to effectively manage the electric field stress on the 132 kV ICA.

IX. Trials and Installation

Following a successful mechanical trial which lasted for two years, up to 2012 [19], a live testing facility was commissioned within a substation near the Northeast coast of Scotland. There, two 400 kV insulating cross-arms have been installed, both using the aforementioned HV and grounded end grading devices. The trial aims to observe the electrical behavior of the cross-arm by monitoring in real time the leakage current of the insulating members, help identify ageing trends and inform the optimization of future designs [20].

In August 2013 six 132 kV insulating cross-arms employing the grading devices described earlier were manufactured and installed on a live line in Scotland (Fig. 12). These have since been operating without incident.

TABLE II
Corona Extinction Voltage

	Observed (kV)	Corrected (kV)
1	165.0	165.3
2	178.0	178.4
3	177.0	177.4
Average	173.0	**173.7**

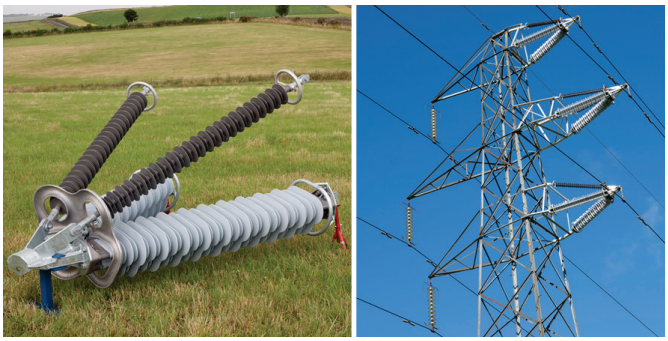

Fig. 12. Assembled 132 kV ICA (left) and three ICAs installed on one circuit of a 132 kV Scottish and Southern Energy Power Distribution line (right).

X. Discussion

After tackling the various challenges presented by this study, the following recommendations have been drawn which can be applied to similar future studies:

1. The construction of the mesh is of critical importance for the validity of the simulation results since a sharp point can greatly increase the reported value of the electric field magnitude. Particular attention should be given to maintaining a good mesh quality to avoid inverted elements and singularities. Also by using at least two second-order elements per 90° arc the discretization error can be kept below 0.1%. To achieve the above, it is likely that some model entities might require meshing with manually defined parameters.
2. Since it is not possible to define an infinite surrounding air domain, its dimensions play an important part concerning the accuracy of the results. If the zero charge boundaries are too close to the electric potential boundaries the electric field computation will be erroneous. To avoid this, a separate simulation incorporating only the metallic hardware can be performed beforehand.
3. The majority of FEA studies presented in existing literature take advantage of the inherent rotational symmetry present in conventional OHL insulators to reduce the complexity and time required for the computation. Consequently, most of the studies are two dimensional. Simulations in two dimensions are a good starting point for electric field analysis but care should be taken to not over-simplify the models. In the case of composite cross-arms three-dimensional models have been found to be necessary to achieve satisfactory results.
4. Using FEA in three dimensions rather than two, requires a great increase in the number of finite elements. As a result, and because of the memory limitations of current computing hardware, other associated components such as the conductor, the conductor shoe and the tower can be omitted or simplified. In the case of the ICA this did not affect the results of the analysis but such simplifications should only be performed after careful study of their effects.
5. Design limits that have been established for the electric field magnitude are based on sound theoretical principles and well documented research. However, often published details concerning FEA studies are vague at best and

methods are not included in international standards. A set of clear guidelines is required so that FEA studies can produce meaningful results that can be used to compare the performance of different solutions with consistency.

XI. Conclusion

The use of FEA has been proven to be particularly efficient for designing electric field stress control devices for the ICA, helping to overcome many of the challenges created by the unconventional shape of the compression insulator and the size of the assembly. By modelling all the major parts of the ICA and computing the electric field using FEA, the areas of high electric field enhancement were identified and the design of the grading devices greatly accelerated. The grading devices developed using this methodology have been shown to work as intended by both laboratory testing and by successful installations in the field.

The innovative design of the HV grading device [21] would not have been possible without extensive use of the FEA method. A set of recommendations is given in the Discussion for designers working with complex insulating structures.

Acknowledgment

The authors would like to acknowledge the support of Scottish and Southern Energy Power Distribution and National Grid. Many people contributed to making this design a reality: Special thanks to Frank Allison, Peter Rhodes, Alistair MacLeod and John Baker for their contributions on the way.

References

[1] S. M. Rowland, R. MacLaren, I. Cotton, D. Chambers, V. Peesapati, and C. Zachariades, "Development of insulating cross-arms for compact HV lattice tower structures," *CIGRÉ Session 2014,* vol. SC B2-107, 2014.

[2] D. Stefanini, J. M. Seifert, M. Clemens, and D. Weida, "Three dimensional FEM electrical field calculations for EHV composite insulator strings," *Power Modulator and High Voltage Conference (IPMHVC), 2010 IEEE International*, 2010, pp. 238-242.

[3] A. J. Phillips, J. Kuffel, A. Baker, J. Burnham, A. Carreira, E. Cherney, W. Chisholm, M. Farzaneh, R. Gemignani, A. Gillespie, T. Grisham, R. Hill, T. Saha, B. Vancia, and J. Yu, "Electric Fields on AC Composite Transmission Line Insulators," *Power Delivery, IEEE Transactions on,* vol. 23, pp. 823-830, 2008.

[4] A. J. Phillips, D. J. Childs, and H. M. Schneider, "Aging of nonceramic insulators due to corona from water drops," *Power Delivery, IEEE Transactions on,* vol. 14, pp. 1081-1089, 1999.

[5] Z. Yong, K. Haji, M. Otsubo, and C. Honda, "Surface Degradation of Silicone Rubber Exposed to Corona Discharge," *Plasma Science, IEEE Transactions on,* vol. 34, pp. 1094-1098, 2006.

[6] A. J. Phillips, D. J. Childs, and H. M. Schneider, "Water drop corona effects on full-scale 500 kV non-ceramic insulators," *Power Delivery, IEEE Transactions on,* vol. 14, pp. 258-265, 1999.

[7] S. Wright and D. Dumora, "Design criteria for composite insulators," *Non-Ceramic Insulators for Overhead Lines, IEE Colloquium on*, 1992, pp. 4/1-4/4.

[8] K. Sokolija, M. Kapetanovic, R. Hartings, and M. Hajro, "Considerations on the Design of Composite Suspension Insulators Based on Experience from Natural Ageing Testing and Electric Field Calculations," *CIGRÉ Session 2000,* vol. 33-204, 2000.

[9] V. M. Moreno and R. S. Gorur, "Impact of corona on the long-term performance of nonceramic insulators," *Dielectrics and Electrical Insulation, IEEE Transactions on,* vol. 10, pp. 80-95, 2003.

[10] K. Sokolija and M. Kapetanovic, "About some important items of composite insulators design," *High Voltage Engineering, 1999. Eleventh International Symposium on (Conf. Publ. No. 467)*, 1999, pp. 284-287 vol.4.

[11] L. Qi, S. M. Rowland, and R. Shuttleworth, "Calculating the Surface Potential Gradient of Overhead Line Conductors," *Power Delivery, IEEE Transactions on,* vol. 30, pp. 43-52, 2015.

[12] National Grid, "Technical Specification - Composite Insulators for Overhead Lines," *TS 3.4.18*, ed, 2008.

[13] EPRI, *AC Transmission Line Reference Book - 200 kV and Above*, 3rd ed. Palo Alto: Electrical Power Research Institude, 2005.

[14] P. M. Kurowski, *Finite Element Analysis for Design Engineers*. Warrendale, USA: Society of Automotive Engineers, Inc., 2004.

[15] O. C. Zienkiewicz, R. L. Taylor, and J. Z. Zhu, *Finite Element Method - Its Basis and Fundamentals*, 6th ed. Barcelona, Spain: Elsevier, 2005.

[16] W. Frei. (2013). *Meshing Considerations for Linear Static Problems*. Available: http://www.uk.comsol.com/blogs/meshing-considerations-linear-static-problems/

[17] National Grid, "Technical Specification - Insulator Sets for Overhead Lines," *TS 3.4.17*, ed, 2006.

[18] The British Standards Institution, "High-voltage test techniques - Part 1: General definitions and test requirements," *BS EN 60060-1*, ed, 2010.

[19] C. Zachariades, S. M. Rowland, I. Cotton, P. R. Green, C. A. Veerappan, and D. Chambers, "A Trial Installation of High Voltage Composite Cross-arms," *XVII International Symposium on High Voltage Engineering*, Hannover, Germany, 2011.

[20] C. Zachariades, I. Cotton, S. M. Rowland, V. Peesapati, P. R. Green, D. Chambers, and M. Queen, "A coastal trial facility for high voltage composite cross-arms," *Electrical Insulation (ISEI), Conference Record of the 2012 IEEE International Symposium on*, 2012, pp. 78-82.

[21] S. M. Rowland, V. Peesapati, C. Zachariades, I. Cotton, P. D. Rhodes, and D. Chambers, "A Grading Device," United Kingdom Patent WO2013171503, 2013.

Christos Zachariades was born in Athens, Greece, in 1984. He received the BEng (Hons) in electrical and electronic engineering from the University of Manchester, UK, in 2009, the MSc in electrical power systems engineering from the University of Manchester in 2010 and the PhD in electrical and electronic engineering from the University of Manchester, in 2014.

Since 2014, he has been working as a Development Engineer and Knowledge Transfer Partnership Associate on a collaborative project between High Voltage Partial Discharge and the University of Manchester.

Dr. Zachariades is a member of the Institution of Engineering and Technology (IET) and a member of the Cyprus Scientific and Technical Chamber (ETEK).

Simon M. Rowland (SM'07) was born in London, England. He completed the B.Sc. degree in physics at The University of East Anglia, and the PhD degree at London University, UK.

He has worked for many years on dielectrics and their applications and has also been Technical Director within multinational companies. He joined The School of Electrical

and Electronic Engineering in The University of Manchester in 2003, and was appointed Professor of Electrical Materials in 2009, and Head of School in 2015.

Prof. Rowland was President of the IEEE Dielectric and Electrical Insulation Society from 2011-12.

Ian Cotton (SM) studied Electrical Engineering at the University of Sheffield. Following this he worked for an electricity distribution company before returning to University to complete a PhD on lightning protection of wind turbines at UMIST.

Since 1998 he has been with the School of Electrical and Electronic Engineering at the University of Manchester. His research has led to a number of patents and the formation of a spin-off company, Arago Technology, of which he is a Director.

Prof. Cotton is also the Director of Manchester Energy, the cross-University research initiative maximising the societal impact of our energy research.

Vidyadhar Peesapati was born in Edinburgh, in 1980. He received a degree in electrical and electronics engineering from the University of Madras, in 2001, the MSc in electrical power engineering from the University of Manchester, in 2006 and the PhD from the University of Manchester, United Kingdom, in 2010.

He is currently a Knowledge Transfer Fellow in the School of Electrical and Electronic Engineering, University of Manchester.

David Chambers graduated from The University of Nottingham in Materials Science. He spent 10 years as an engineer and senior Manager in EPL Composites developing innovative products for a wide range of markets.

He is now managing Director of Arago Technology. He also is a director of Innovation to Industry (I2I), an engineering company that specialises in all aspects of the innovation process.